

Electronic spectroscopy and dynamics of the monomer and Ar_n clusters of 9-phenylfluorene

Jonathan D. Pitts and J. L. Knee^{a)}

Department of Chemistry, Wesleyan University, Middletown, Connecticut 06459

(Received 18 May 1998; accepted 28 July 1998)

The spectrum of the S_1 electronic state of jet-cooled 9-phenylfluorene-Ar_n, $n=0-4$, has been measured by two color resonant enhanced multiphoton ionization spectroscopy. The cation ground states of these complexes have also been studied by mass analyzed threshold ionization (MATI) spectroscopy in a 1+1 excitation process with various intermediate states in S_1 . *Ab initio* calculations in conjunction with the spectroscopy have determined that the phenyl ring at the 9 position is perpendicular to the plane of the fluorene moiety yielding an overall symmetry of C_s . The Ar complexes for $n=1-3$ exhibit multiple isomers which are identified in the S_1 spectrum and confirmed by MATI spectroscopy. The structure of these isomers is determined by spectral analysis and additivity rules as well as atom-atom calculations using a Lennard-Jones potential. Vibrational dynamics from selected S_1 vibronic levels are observed by the appearance of the picosecond or nanosecond time delayed MATI spectra. Vibrational redistribution and dissociation of the clusters are measured with nanosecond and picosecond time resolution. It is found that different isomers of the $n=1$ cluster show dramatically different rates of redistribution for several vibronic bands.

© 1998 American Institute of Physics. [S0021-9606(98)00641-2]

I. INTRODUCTION

In the study of molecular clusters, structure is perhaps the most fundamental property and is central to understanding any reactivity and dynamics which may occur. A very large effort using microwave,¹ infrared,² and high resolution electronic spectroscopy³ has provided a great database of structures for all kinds of weakly bound complexes in both ground and excited states. The vast majority of these clusters are formed at very low temperatures in supersonic molecular beams. The beam conditions allow formation of the complexes but the details of the kinetics of cluster formation are not completely understood and the distribution of cluster isomers is not easily predicted. We will consider here clusters of aromatic molecules with argon.

Multiple cluster conformations have been identified in aromatic-Ar_n clusters, but almost exclusively when $n > 1$. Examples of multiple conformations are anthracene-Ar_n,^{4,5} tetrazene-Ar_n,⁶ benzene-Ar_n,⁷ and others.⁸⁻¹³ Recently we have extensively studied two distinct conformational isomers of fluorene-Ar₄, where the distinct nature of the (2|2) and (3|1) species was confirmed using pump-probe zero electron kinetic energy (ZEKE) photoelectron spectroscopy.^{14,15} Nanosecond and picosecond experiments were applied to measure the dynamical interconversion of these species.

While multiple isomers for $n > 1$ species are common, multiple isomers for $n = 1$ species are rare,¹⁶ particularly for aromatic-Ar species. In almost all cases simple atom-atom calculations show multiple minima for the Ar₁ species. The reliability of these calculations has been confirmed repeatedly so the existence of multiple minima is quite certain. The question is then the population of these minima and the cri-

teria which determine these populations. Multiple conformational minima in covalently bound molecules, such as cis/trans conformations¹⁷ in 1-naphthol and axial/equatorial in 4-methylcyclohexanone,¹⁸ are often seen in jet cooled molecules with the Boltzmann ratios of the populations being nearer room temperature than the very low rotational/vibrational temperatures measured in the jet. In these cases the non-Boltzmann populations of conformations are ascribed to large barriers for interconversion which cannot be overcome in the jet cooling process.

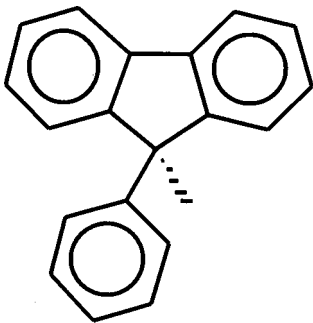
On the other hand, the barriers between different isomers in weakly bound complexes can be quite small. Consider naphthalene-Ar where there are two minima with the Ar centered above one of the two rings in this symmetric system. Simple calculations¹⁹ have shown that the barrier between these minima is less than 1 cm⁻¹. Clearly the calculations do not have this level of accuracy but it demonstrates the small barriers which may occur, making it very likely that clusters will be cooled to the lowest energy isomer in supersonic expansions.

Side crossing transitions represent a somewhat larger barrier to isomer interconversion. For instance, in fluorene-Ar¹⁵ the side crossing barrier between the two equivalent minima is 260 cm⁻¹. This may lead to different isomers, although most of the aromatic molecules studied to date have planar symmetry and thus distinction of isomers on either side of the molecules is impossible. Similarly, the ground vibrational state may be above the barrier, resulting in effectively one conformation.

With these factors in mind we have purposely chosen 9-phenylfluorene-Ar_n (PF-Ar_n) for study. Distinct isomers seemed more likely here for two reasons. First there is an asymmetry with respect to the plane of the aromatic system so that binding sites "above" and "below" the plane of the

^{a)}Electronic mail: jknee@wesleyan.edu

fluorene are distinct. Second, the phenyl substituent could perhaps provide an additional binding site. In fact, our predictions were borne out and two distinct isomers are observed for the Ar_1 complex which we have assigned to argon being above and below the fluorene. We take advantage of this situation to measure the isomer specific intramolecular vibrational redistribution (IVR) and dissociation dynamics of the PF-Ar_1 complex.



II. EXPERIMENT

A detailed description of the experimental apparatus has been given elsewhere,^{14,15} so only a brief synopsis is given here. Two color 1+1 resonantly enhanced multiphoton ionization (REMPI) spectroscopy with mass resolved detection is used to study the spectroscopy of the S_1 electronic state of the jet cooled clusters. Mass analyzed threshold ionization (MATI) spectroscopy,²⁰ the mass resolved equivalent of zero electron kinetic energy (ZEKE) spectroscopy, is used for the photoelectron spectroscopy of the ion ground state. References 14, 15, 21, and 22 give a complete description of our application of ZEKE and MATI to the study of molecular clusters.

Nanosecond and picosecond laser systems were separately used in this study. The nanosecond laser system employed in these experiments consists of two dye lasers (Lumonics HD-500) pumped by the second harmonic of a pulsed Nd:yttrium-aluminum-garnet (YAG) (Continuum NY-61) operating at 20 Hz. The visible output of each dye laser has a pulse width of 6 ns and a bandwidth of 0.04 cm^{-1} . Both dye lasers are frequency doubled and one functions as the pump and the other as the probe. The pump and probe lasers were temporally overlapped by an appropriate optical delay and spatially overlapped in the vacuum chamber under slightly focused conditions. Care was taken to minimize any signal from either laser alone. The second laser system, used for time resolved studies, is a pulse amplified picosecond system. This consists of a continuous wave mode-locked Nd:YAG (Coherent Antares) synchronously pumping two dye lasers. Each dye laser is amplified in separate three stage dye amplifiers, pumped by the second harmonic of a Nd:YAG regenerative amplifier (Continuum RGA-67) operating at 20 Hz. The amplified output pulse width is $\sim 15 \text{ ps}$ with a bandwidth of 5 cm^{-1} and an energy of $0.2\text{--}1 \text{ mJ/pulse}$ in the visible. The overall cross correlation is $>20 \text{ ps}$ due to jitter between the two dye lasers. Laser wavelengths were calibrated with a Na/K/Ne hollow cathode lamp.

A pulsed supersonic beam originates in the first of two differentially pumped chambers. The nozzle has a sample container which holds the phenylfluorene (PF) sample (Aldrich) and is heated to $130\text{--}150 \text{ }^\circ\text{C}$. The exact vapor pressure is unknown but we estimate it as significantly below 1 Torr. For complexation of PF with Ar, a mixture of 10% Ar in He or Ar in Ne was used in the expansion. The backing pressure was varied from 1.4 to 2.5 bar in order to optimize the desired clusters. The pulsed beam is skimmed and enters the second chamber where the spectroscopy takes place.

The REMPI spectra were obtained by fixing the probe slightly higher than the ionization potential of the complex and scanning the pump. Probe energy and intensity were adjusted to avoid any dissociation from higher clusters. The MATI spectra were obtained by fixing the pump to the S_1 vibronic band of interest and scanning the probe through the ionization potential (IP). The MATI spectra were somewhat difficult to obtain due to the challenge of separating the prompt background ions from the Rydbergs of interest. To achieve clean separation of the prompt and MATI signals, we implemented a pulsed Wiley-McClaren²³ extraction scheme in which the upper grid pulse width was varied to act as a mass filter. In this way the contribution from the cluster and fragments, other than the one of interest, could be eliminated. The MATI scheme used a delayed discrimination field of -2 V/cm and an extraction pulse of 560 V/cm which was delayed $\geq 15 \text{ } \mu\text{s}$. The ions then traverse the time of flight (TOF) mass spectrometer and are detected on dual stack microchannel plates (Galileo Electro-Optic Corp).

Time resolved data was obtained in two ways. A crude measure of the dynamics was obtained by using the nanosecond laser system and measuring MATI spectra at early and late time delays. The early time spectra were obtained with a probe optical delay such that the pump and probe pulses were temporally overlapped to within $\pm 0.5 \text{ ns}$. The pulse widths are 6 ns, so clearly this is a convolution of a rather large time window. The late time spectra were obtained by delaying the probe by 7 ns. This approach was effective in revealing dynamic structure in the MATI spectra but could not quantify any decay times. A more precise measure of the dynamics was obtained by using the picosecond laser system and a computer controlled optical delay line. The dynamics were then recorded as a change in the MATI signal as a function of the delay line position. While this was more accurate, the picosecond measurements suffered from lack of sensitivity.

III. RESULTS

A. Calculations of PF monomer structure

We report first the calculated structure of PF since the structure will be the basis for analyzing the spectroscopy. In considering the overall structure, it is clear that the fluorene and phenyl moieties are likely to be very close to the respective parent molecules with the major question then being the relative orientation of the two ring systems. This orientation is critical for consideration of the structure of the Ar complexes since it should affect the ability of Ar to interact with the various faces of the aromatic moieties.

To obtain the PF structure, two *ab initio* calculations were performed with GAUSSIAN 94.²⁴ The first was a complete optimization at the Hartree–Fock (HF) level using a 6–31 G(d) basis set. This simple calculation predicts that the phenyl moiety is perpendicular to the plane of the fluorene (C_s symmetry). In order to gain confidence in this low level calculation, the PF was also optimized using the density functional method Becke–3–Lee–Yang–Parr (B3LYP).²⁵ The same 6–31 G(d) basis set was used. This higher level calculation also predicts that the phenyl group is perpendicular to the fluorene plane. These calculations can be compared to the published x-ray crystal structure of PF.²⁶ This crystal structure has a 104° angle between the planes of the fluorene and phenyl as compared to the calculated value of 90° . We ascribe this modest difference to crystal packing interactions. The other bond angles and bond lengths are in close agreement between the crystal structure and the calculated values.

The vibrational frequencies were also calculated with a particular interest in calculating the phenyl torsion for comparison with several observed low frequency modes. Due to computational limitations, the calculation was only run at the HF level with a 6–31 G(d) basis set. The four lowest calculated frequencies (scaled by 0.893) were 79.5, 98, 98, and 128 cm^{-1} . The third mode at 98 cm^{-1} is identified as essentially a pure torsion. These results will be discussed below with the analysis of the observed spectrum.

B. Calculation of PF–Ar_n structure

In order to determine the possible structures, and relative energies, of the various isomers of 9-phenylfluorene–Ar_n, a series of calculations were performed. The details of these types of calculations have been described elsewhere,¹⁵ so only a short summary is given here.

The HYPERCHEM²⁷ package was used to perform a series of annealing and geometry optimizations for various cluster sizes. A simple pairwise Lennard-Jones potential was used to describe all interactions between the argons and the chromophore. The values of these parameters are given in Ref. 14. To confidently predict all local minima, the 9-phenylfluorene is held static at its calculated conformation, while the argons are heated in a range of 50–150 K. The temperature is chosen to provide adequate sampling of the phase space. After each annealing process the perturbed structure is geometry optimized. Each cluster undergoes hundreds of annealing processes, with varied starting conditions, so that we can confidently find all local minimum structures.

The numerical results of these calculations are given in Table I and the resulting structures are shown in Fig. 1. In the case of $n = 1$, two isomers are found. The lowest energy conformation (isomer Ia) has the argon localized near one of the aromatic rings in the fluorene segment and on the same side as the phenyl ring. The second isomer (isomer Ib) is similar to the fluorene–Ar case,¹⁴ with the argon situated over the center ring of the fluorene, and on the side opposite the phenyl moiety. For the $n = 2$ complex, four isomers are predicted. In order of increasing energy they are, both argons on the phenyl side of PF with one localized near a benzene ring, and one closer to the phenyl substituent (isomer IIa).

TABLE I. Summary of cluster minimum energies with a Lennard-Jones potential.

| Cluster | Isomer | Energy (kcal/mol) ^a | Energy (cm ⁻¹) ^a |
|--------------------|-----------------------------|--------------------------------|---|
| PF–Ar | Ia | –1.66 | –581 |
| | Ib | –1.49 | –521 |
| PF–Ar ₂ | IIa | –3.47 | –1214 |
| | IIb | –3.34 | –1168 |
| | IIc | –3.16 | –1105 |
| | 2 0 ^b | –3.11 | –1088 |
| PF–Ar ₃ | IIIa | –5.17 | –1808 |
| | IIIb | –4.98 | –1742 |
| | IIIc | –4.85 | –1697 |
| | Symmetric 3 0 ^b | –5.38 | –1882 |
| | 3 0 ^b | –5.30 | –1854 |
| | Asymmetric 2 1 ^b | –4.95 | –1732 |
| | 0 3 ^b | –4.74 | –1658 |

^aRelative to the monomer energy (0.00 kcal/mol).

^bNumbers to the left of | represent argons on the same side as the phenyl moiety. Numbers to the right of | represent argons on the side opposite the phenyl moiety.

The next is a symmetric structure with both argons located over the two aromatic rings in the fluorene segment (isomer IIb) on the phenyl side of the molecule. The third is the (1|1) isomer (IIc), and the fourth the (0|2) isomer with both being located on the side opposite the phenyl substituent. It is unlikely that this highest energy isomer exists in our supersonic expansion since we did not see it in the case of fluorene–Ar₂.¹⁴ For the cluster containing three argons, again three low energy isomers are calculated. They are seen in Fig. 1

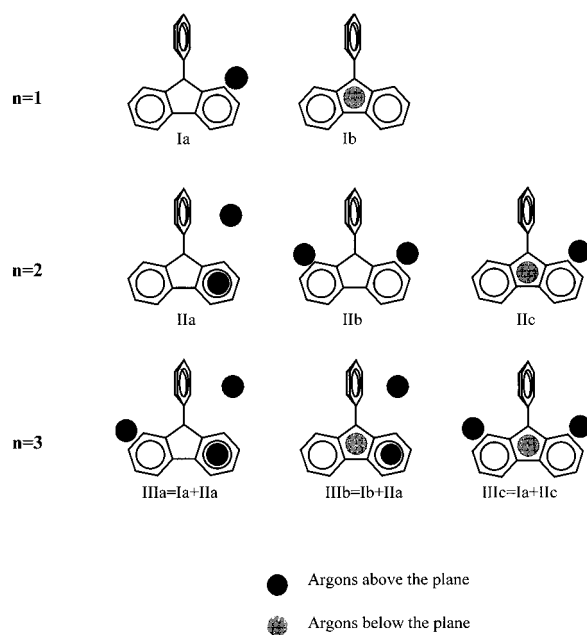


FIG. 1. Schematic representations of the ethylfluorene–Ar_n isomeric structures calculated with simple Lennard-Jones atom–atom calculations. The black disks represent the argon position above the plane (on the same side as the phenyl substituent) and the gray disk represents argon below the fluorene plane. The isomer labels are used throughout the text. Energetic details of these structures are given in Table I.

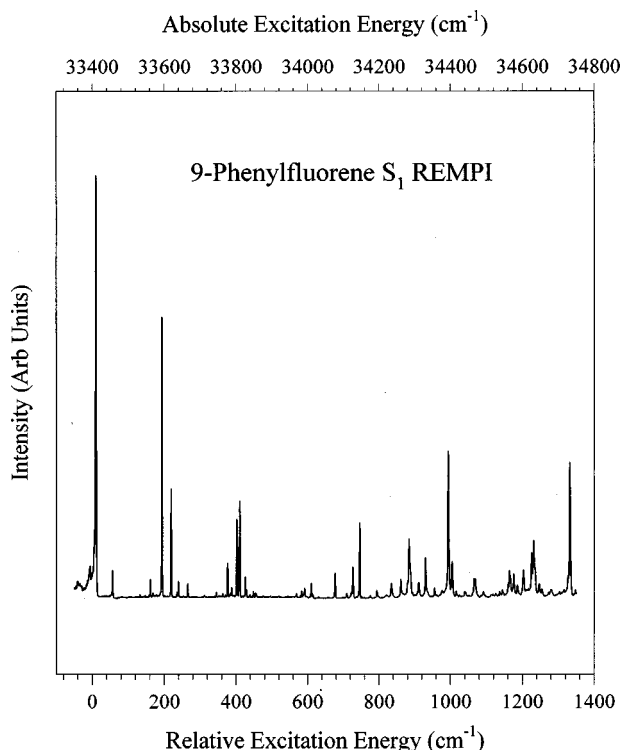


FIG. 2. Two color, mass gated, resonant enhanced multiphoton ionization (REMPI) spectrum of 9-phenylfluorene. The spectrum is not normalized and consists of several different scans. The weaker pump laser is scanned as indicated, while the more intense probe is fixed above the ionization threshold at $29\,700\text{ cm}^{-1}$. The lower axis is relative to the origin at $33\,410\text{ cm}^{-1}$.

and are comprised of combinations of the $n=1$ and $n=2$ calculated structures. As one would expect, the lowest energy $n=3$ isomer is a combination of the lowest $n=1$ and $n=2$ isomers (i.e., IIIa=Ia+IIa). It is important to note that the calculations predict several (3|0) isomers as seen in Table I. It is convenient to think of the lowest energy structure as static, but it is more likely that some sampling of structures similar in energy does occur. The next lowest (isomer IIIb) is a combination of Ib and IIa. The highest energy conformation pertinent here is the symmetric $n=3$. It again follows from the combination of $n=1$ and $n=2$ conformations, noted here as IIIc which equals Ia+IIc. As is the case in the Ar_2 , the $n=3$ isomer with all argons on the side opposite the phenyl is not likely since it is not observed in the fluorene- Ar_3 complex.¹⁴

These calculations alone cannot necessarily predict the correct observed structures but are extremely useful, in conjunction with the spectroscopic observables, in guiding the interpretation of the data.

C. PF monomer spectroscopy

To the best of our knowledge, detailed gas phase electronic spectroscopy of PF has not been reported. We report here the jet-cooled spectra of the S_1 electronic state obtained via two color REMPI experiments outlined above. The monomer spectrum from the origin ($33\,410\text{ cm}^{-1}$) to 1330 cm^{-1} excess energy is shown in Fig. 2. A complete analysis of the spectrum has not been undertaken, but some key points will be noted. In the energy region scanned there are a

number of stronger bands which can be associated with similar structure in the fluorene molecule. Several other new bands arise and these are associated with the addition of the phenyl substituent.

The symmetry of PF, based on the above calculations, is C_s . In fluorene the S_1 state has B_2 symmetry in C_{2v} point group. Assuming the electronic excitation is only slightly changed in PF, this would yield A'' for the excited electronic state symmetry. Most of the vibrations observed in fluorene have a_1 symmetry which would be a' in PF and these are the bands we expect to observe. The major bands of interest in PF are at 184, 209, 392, 400, and 738 cm^{-1} . The 184 cm^{-1} band correlates with the 208 cm^{-1} band in fluorene which is assigned as an a' fundamental consisting of motions involving in-plane CCC bends and the scissor motion of the aliphatic CH_2 group. This mode has a calculated scaled frequency of 200 cm^{-1} in the ground state. The decrease in frequency of this mode with phenyl substitution is expected due to the mass effect. The band at 209 cm^{-1} has approximately half the intensity of the 184 cm^{-1} band but has no direct counterpart in the observed fluorene spectrum. The calculations do not reveal a band in this region to assign as a fundamental, so a possible assignment is the overtone of the phenyl torsion which is calculated to be at 195 cm^{-1} . The strong band observed at 392 cm^{-1} correlates with the 398 cm^{-1} band in fluorene and has a calculated ground state frequency in PF of 398 cm^{-1} . This band is primarily a CCC in-plane stretch. The observed 738 cm^{-1} band in PF correlates with the 722 cm^{-1} band in fluorene and is assigned as an in-plane CCC and CH bend motion. The calculated ν_{26} mode has a similar motion and a ground state scaled frequency of 735 cm^{-1} .

Many MATI spectra of the monomer were recorded with numerous S_1 intermediate states in the 1+1 excitation scheme. Due to the very strong $\Delta v=0$ propensity rule, the spectra were only scanned in a narrow frequency range with the intent to measure the vibrational frequencies in the cation.

D. PF- Ar_n spectra and isomer assignments

The S_1 and MATI spectra have been recorded for the $n=1-4$ complexes. These will be discussed in some detail since they are central to the dynamics studies. The spectra in the S_1 origin region are shown in Fig. 3 and the origin locations are listed in Table II. These spectra were obtained by two color mass resolved REMPI experiments with mass gating on the respective peaks. The laser powers were adjusted to minimize signal from each laser alone and the probe laser was tuned just above the IP to limit fragmentation. It is immediately obvious that the interpretation has some subtlety since the strongest peak in each cluster spectrum does not appear as the reddest feature. Also one can see that the reddest peak of the $n=1$ is nearly coincident with the second reddest of the $n=2$ and the third reddest of the $n=3$. This is very suggestive of cluster fragmentation but this was rigorously eliminated, as mentioned above, and also checked with MATI spectroscopy as discussed below. The two reddest bands of the $n=1$ cluster, located at -25 and -47 cm^{-1} ,

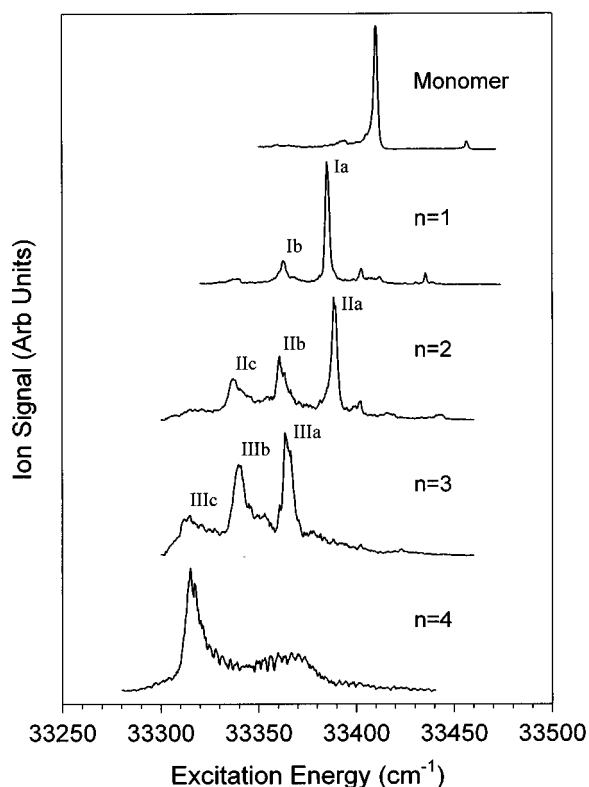


FIG. 3. Two color, mass gated, resonant enhanced multiphoton ionization (REMPI) spectra of 9-phenylfluorene- Ar_n complexes, $n=0-4$, in the region of the electronic origin. The peaks are labeled with the isomer assignments; see Fig. 1.

with respect to the monomer are in fact two different isomers. The $n=2$ and $n=3$ complexes each exhibit three isomers and the origin values are listed in Table II. The assignment of the bands to separate isomers was unambiguously determined by the MATI spectroscopy which showed that each isomer has a unique ionization potential and distinct photoelectron spectrum. The ionization potential data are also summarized in Table II.

It is tempting to use the isomer peak intensities with a Boltzmann population analysis to assign relative isomer stabilities. However, given the uncertainty in the isomer cooling process and the kinetic considerations which may be in-

TABLE II. Phenyl fluorene- Ar_n spectral data.

| Species | S_1 origin ^a | ΔS_1^b | $S_1 \rightarrow \text{ion}$ | $\Delta S_1 \rightarrow \text{ion}^b$ | IP | ΔIP^b |
|------------|---------------------------|----------------|------------------------------|---------------------------------------|--------|----------------------|
| $n=0$ | 33 410 | ... | 29 580 | ... | 62 990 | ... |
| $n=1$ Ia | 33 385 | -25 | 29 579 | -1 | 62 964 | -26 |
| Ib | 33 363 | -47 | 29 548 | -32 | 62 911 | -79 |
| $n=2$ IIa | 33 389 | -21 | 29 540 | -40 | 62 929 | -61 |
| IIb | 33 361 | -49 | 29 540 | -40 | 62 901 | -89 |
| IIc | 33 337 | -73 | 29 548 | -32 | 62 885 | -105 |
| $n=3$ IIIa | 33 365 | -45 | 29 506 | -74 | 62 871 | -119 |
| IIIb | 33 340 | -70 | 29 510 | -70 | 62 850 | -140 |
| IIIc | 33 315 | -95 | 29 507 | -73 | 62 822 | -168 |
| $n=4$ | 33 315 | -95 | 29 477 | -103 | 62 792 | -198 |

^aAll values reported in the table are in cm^{-1} .

^bNumbers are reported relative to the corresponding values in the monomer.

olved, we have little confidence that the populations are equilibrated and so do not include peak intensities in our analysis.

1. $n=1$

Having established that the spectral peaks represent distinct isomers, the assignment of particular structures to the spectral features can be attempted. For the $n=1$ system the calculations show two distinct minima with the argon on either side of the fluorene ring. As discussed above, these are isomers Ia and Ib. For the complex with argon anti to the phenyl substituent, the position is identical to that in fluorene and one would expect a similar shift in the S_0 to S_1 absorption from the monomer of -42 cm^{-1} . In fact, the shift of the red most spectral feature for $n=1$ is -47 cm^{-1} and, based on this similarity, we assign this to isomer Ia. The other, bluer peak, has a shift of -25 cm^{-1} and is assigned as isomer Ib. Further support for these assignments will be added in the discussion of the MATI results and dynamics experiments presented below.

Assignment of the structure of the $n=2$ and 3 complexes is then based on additivity rules. These rules are based on the fact that each argon binding site on the chromophore has associated with it a shift of the electronic absorption and that the overall shift for multiple argons can be obtained by summing the individual shifts. For instance, fluorene- Ar_2 has an argon on each side, centered on the five membered ring. The shift is then expected to be just twice that of the Ar_1 (-45 cm^{-1}) which yields a predicted shift of -90 cm^{-1} which compares closely with the experimental observation of -83 cm^{-1} . If the second Ar goes on the same side as the first (not actually observed in fluorene- Ar_2) the additivity is expected to break down because calculations show that the second Ar displaces the original Ar from the five membered ring to accommodate binding of the second Ar.

2. $n=2$

For $n=2$, three distinct isomers are observed. The reddest peak has a shift of -73 cm^{-1} with respect to the monomer. Using the additivity, we can add the shifts of Ia+Ib, $-43 + -25 = -68$, which compares reasonably with -73 cm^{-1} and thus we assign this reddest feature to structure IIc, Fig. 1. The middle feature is redshifted -45 cm^{-1} which can be approximated by the additivity of Ia+Ia, $-25 + -25 = -50 \text{ cm}^{-1}$. This isomer is noted as IIb. The bluest feature for $n=2$, -22 cm^{-1} , cannot be assigned by additivity and thus we ascribe it to structure IIa based on the calculations. This is the asymmetric (2|0) structure and the nonadditivity of the shift is consistent because addition of the second Ar displaces the first Ar from its preferred position and there are then no $n=1$ structures for reference. The proximity of one Ar near the phenyl ring is consistent with a small shift since interaction with the chromophore is then minimized.

3. $n=3$

Calculations show that the number of possible isomers increases for $n=3$, yet only three spectral bands are observed which appear to be separate isomer origins. Starting with the

reddest peak, -95.5 cm^{-1} , we can use the additivity of IIc + Ia, $-73 + -25 = -98 \text{ cm}^{-1}$, to assign this feature to structure IIIc. The spectral feature at -70.5 cm^{-1} is assigned as IIa + Ib, $-22 + -43 = -65 \text{ cm}^{-1}$, and labeled as IIIb. The $n = 3$ feature at -45 cm^{-1} can be assigned to IIa + Ia, $-22 + -25 = -47 \text{ cm}^{-1}$, which is shown as IIIa.

4. $n=4$

Unlike the smaller clusters, $n=4$ exhibits only a single peak at the S_1 origin, suggesting only a single isomer, although there is a broad background which may be unresolved contributions from other isomers. The S_1 origin is shifted by 95 cm^{-1} with respect to the monomer and this can be assigned as an additivity of IIIa + Ib, $-45 + -47 = -92 \text{ cm}^{-1}$. Thus the $n=4$ structure has a (3|1) geometry which is consistent with a low energy isomer in the calculations.

E. Cluster spectra above the S_1 origin

Two color, mass resolved, REMPI spectra of the PF-Ar $_n$ clusters were obtained above the S_1 origin. This was done for two reasons. First, the spectra are used to determine the binding energies by measuring the vibronic onset of cluster dissociation. Second, they are used to measure the vibronic bands which are candidates for dynamic studies using nanosecond and picosecond pump-probe MATI spectroscopy.

The threshold for Ar dissociation in S_1 is usually determined by scanning the spectrum through the higher energy vibronic bands and gating on the PF-Ar. When the threshold is reached, the PF-Ar $^+$ signal does not usually disappear but begins to have the spectral signature of the PF-Ar $_2$ which is fragmenting into the PF-Ar $^+$ channel. In this particular case there is a subtlety since the PF-Ar Ia isomer is only several wave numbers to the red of the PF-Ar $_2$ IIa isomer. However, this shift was enough to identify the dissociation threshold and was confirmed by MATI spectroscopy where the products of the dissociation were directly identified. The highest bound S_1 level for PF-Ar Ia was 417 cm^{-1} and the lowest unbound S_1 level was 669.3 cm^{-1} . This rather wide range is consistent with the binding energy in FI-Ar and with the calculated S_1 value of 493 cm^{-1} for PF-Ar. The threshold for dissociation of PF-Ar isomer Ib was not bracketed experimentally due to the weakness of the S_1 transitions, but it is expected to be similar to Ia.

For $n=2$ isomer IIa the dissociation was bracketed in a similar manner as described above with the result that loss of one Ar in S_1 was bracketed between the same range as $n=1$. The other $n=2$ isomers were too weak to apply this analysis.

F. Cluster MATI spectra

Many MATI spectra of the complexes were obtained by using different intermediate vibronic resonances in the 1+1 excitation process. Here we will focus on the spectra from the S_1 origins while the excited vibronic bands will be discussed in the context of the dynamics studies. Figure 4 shows the MATI spectra of each cluster size and isomer obtained by pumping the respective S_1 origins as indicated.

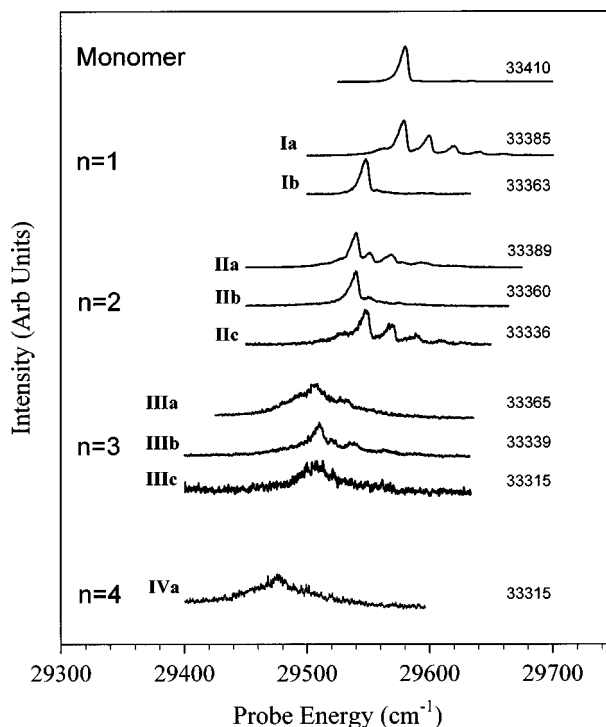


FIG. 4. Mass analyzed threshold ionization (MATI) spectra of 9-phenylfluorene-Ar $_n$ complexes, $n=0-4$, in the region of the cation origin. The data are plotted relative to the probe laser energy. The pump energy for each spectrum is indicated on the right and the cluster size and isomer assignment are indicated on the left.

The ionization potentials are then obtained as the sum of the S_1 and cation threshold and are summarized in Table II.

If one looks at the ionization potentials there is a steady decrease in IP with cluster size with, however, a significant variation among the different isomers. In particular the IPs of isomers Ia and Ib differ by 53 cm^{-1} .

As to the appearance of the MATI spectra, some exhibit low frequency intermolecular bands associated with Ar vibrational motion. For instance $n=1$, isomer Ia, has a pronounced 21 cm^{-1} vibrational progression consistent with an Ar bending motion. The appearance of these modes, and their absence in fluorene-Ar,¹⁴ again supports the assignment of this isomer as having the Ar on the same side as the phenyl as shown in Fig. 1. The other observation to make is the broad nature of the $n=3$ and 4 MATI peaks. This can be ascribed to low frequency hot bands supported in the larger clusters or perhaps additional, unresolved, isomeric structures.

G. Cluster dynamics

The S_1 dynamics of the PF-Ar $_n$ clusters were measured by pump-probe techniques in which an excited vibronic band is excited and a time delayed probe laser is used to monitor the dynamics by measuring the MATI spectrum. Two general types of dynamic processes are expected, namely IVR and unimolecular dissociation. By using a MATI probe, the dissociation channels are easily identified by the mass of the product but can be further refined by also spectrally identifying the state of the reaction product. IVR is identified by

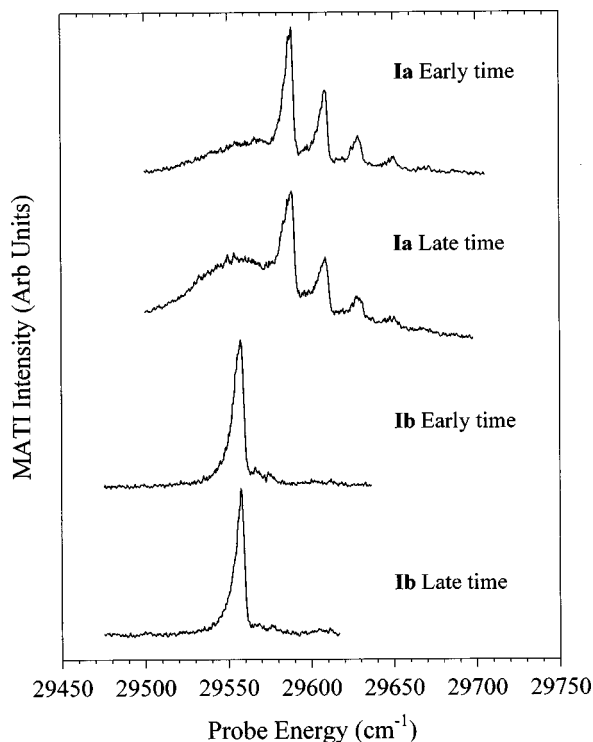


FIG. 5. Nanosecond pump-probe MATI spectra of the 184 cm^{-1} band of the two isomers of PF-Ar_1 at early (~ 0 ns) and late (~ 7 ns) delay time. The spectra are scanned in the region of the $\Delta v = 0$ transition. Isomer Ia clearly shows spectral broadening to the red at late time which is ascribed to vibrational redistribution. Isomer Ib exhibits no spectral changes.

the MATI spectrum in the parent mass channel. The clear signature of IVR is broad MATI peaks centered near the $\Delta v = 0$ transition to the cation.^{14,15,21,28} In cases of multiple isomers it is possible that we can identify isomer interconversion by noting spectral features from different isomers. This was reported¹⁵ for fluorene- Ar_4 in a recent publication and appears to occur upon excitation of the IIb species at the 399 cm^{-1} band.

MATI spectra of the PF-Ar_n clusters were measured at a number of vibronic bands to explore the dynamics. The vibronic intensity is bunched in three regions around 200, 400, and 700 cm^{-1} . The 700 cm^{-1} region is above the bracketed dissociation threshold as discussed above.

1. 200 cm^{-1} region

This region was the most extensively studied and nanosecond and picosecond results are reported for both $n = 1$ and 2. The monomer exhibits prominent bands at 184 and 209 cm^{-1} . Figure 5 shows the nanosecond MATI spectra of the 184 cm^{-1} band for both isomers, Ia and Ib, of the $n = 1$ complex at early and late time. The Ia isomer spectra clearly show a change in time with significant broad, redshifted structure coming in at the expense of the sharp, blueshifted resonance. The sharp band is assigned as the $\Delta v = 0$ transition to the cation 184 cm^{-1} band (shifted to 181 cm^{-1} in the cation based on monomer studies). The broad structure is a result of IVR which populates the low frequency intermolecular modes. It should be noted for future reference that the broad structure is centered at 29555 cm^{-1} which is red-

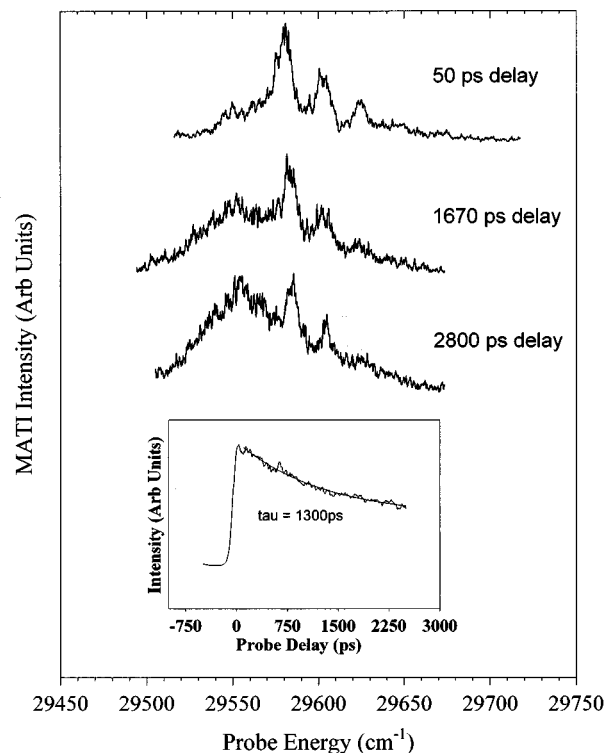


FIG. 6. Picosecond time resolved pump-probe MATI spectrum pumping the 184 cm^{-1} band of PF-Ar_1 , isomer Ia. The inset shows the time decay behavior when probing the sharp structure in the spectrum.

shifted by 24 cm^{-1} relative to the expected $n = 1$ $\Delta v = 0$ transition at 29579 cm^{-1} . The redshift is ascribed to decreases in frequency of the intermolecular modes in the cation. Similar behavior has been documented for numerous other systems.^{14,15,21,28} By contrast, isomer Ib shows no change in time at all with only a sharp peak indicating no IVR occurs. This is a striking example of isomer specific dynamics.

The Ia isomer of this band was studied with picosecond excitation and probing. Figure 6 shows the transient behavior measured by gating on the reactant (sharp peak). The decay time constant was fit to ~ 1300 ps, while the rise of the product was fit to ~ 700 ps. Based on our understanding of the system and the model dynamics,^{4,29,30} these time constants should be equivalent, but repeated scans and fitting showed a significant, persistent discrepancy. Analysis based on integrated spectral areas at different time delay agrees with the longer 1300 ps value. Isomer Ib was not scanned with picosecond excitation due to the lack of even nanosecond time scale decay. It should be noted that the overall fluorescence lifetime of this molecule is not known but is expected to be similar to fluorene which is 18 ns.³¹

Two smaller bands in this region appeared in the $n = 1$ S_1 spectrum and are assigned as 205 and 215 cm^{-1} bands for isomer Ia. Nanosecond MATI spectra were obtained for each of these bands pumping at early and late time and are shown in Fig. 7. The 205 cm^{-1} band shows sharp structure at early time (the position of which confirms the assignment to isomer Ia) but is almost completely redistributed at later time. By contrast, the 215 cm^{-1} band shows no sharp structure at

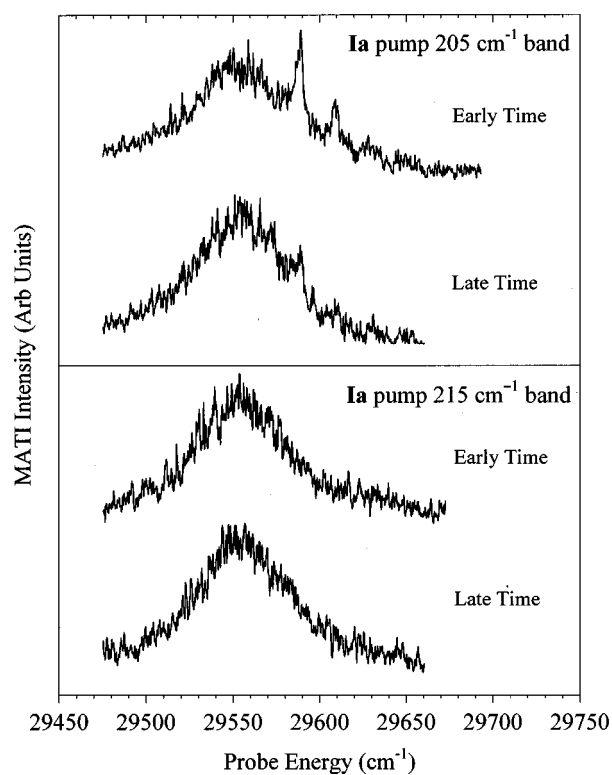


FIG. 7. Nanosecond pump-probe MATI spectra comparing the 205 and 215 cm^{-1} bands of the Ia isomer at early and late time. The residual sharp structure of the 205 cm^{-1} band indicates a slower rate for vibrational redistribution.

any delay, indicating very rapid IVR. Thus, for isomer Ia there is a significant change in redistribution rates between 184 and 205 cm^{-1} and even between 205 and 215 cm^{-1} . The particular identity of these two bands is somewhat of a puzzle. They are symmetrically disposed about an expected band position of 209 cm^{-1} based on the monomer spectroscopy. Also, they have equal intensity of about half of what would be expected for the 209 cm^{-1} band. It would appear that this is a splitting due to the presence of the Ar and may be consistent with the assignment of this band as the overtone of the phenyl torsion. No definitive determination of the nature of these bands has yet been made.

The $n=2$ species are considerably weaker but MATI spectra were scanned for the 184 cm^{-1} band at early time for each of the three $n=2$ isomers. The results showed that redistribution had occurred, to some extent, but there was still residual sharp structure. Picosecond spectra were obtained for the 184 cm^{-1} band of isomer IIa and revealed that the redistribution was complete within 600 ps. No further analysis of the $n=2$ dynamics has been made except for the dissociation behavior at higher energy which is enumerated below.

2. 400 cm^{-1} region

This region shows a number of closely spaced bands which were somewhat difficult to sort out for the $n=1$ complex due to the two conformers present. Careful analysis in fact revealed only one band which was clearly identified as due to isomer Ib, and that is the 399 cm^{-1} band. The other

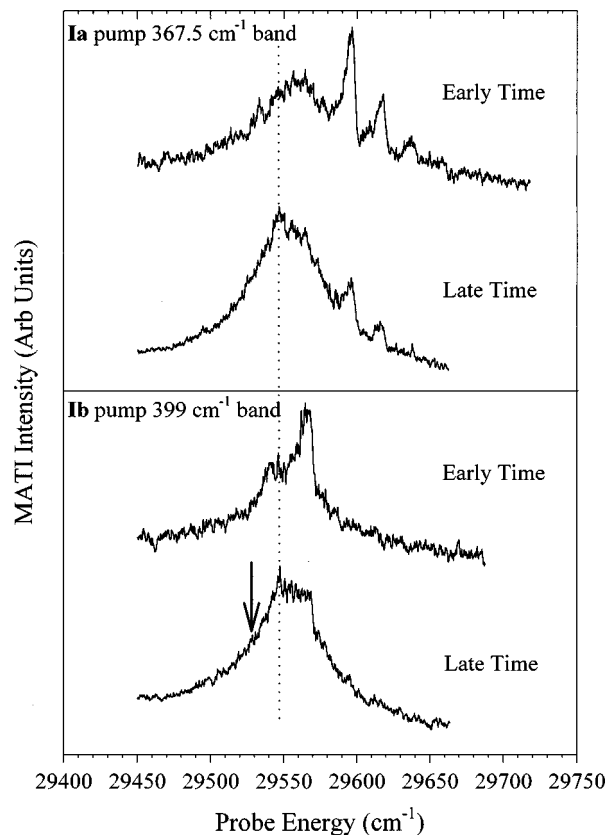


FIG. 8. Nanosecond pump-probe MATI spectra comparing the 367.5 cm^{-1} band of isomer Ia with the 399 cm^{-1} band of isomer Ib, at early and late time. The dotted line is the center of the redistributed structure for Ia, while the arrow indicates where the redistributed structure would be expected for Ib. The similarity of the late time spectra suggests that conformer interconversion is occurring.

significant $n=1$ peaks for which MATI spectra were obtained are assigned to the Ia isomer and appear at 367.5, 381, 388.5, 399, and 416.5 cm^{-1} . Careful REMPI spectra revealed that the complexes are bound for all vibrations in this region. The MATI spectra of all of these bands, except one, are essentially identical and show broad peaks centered at 29 555 cm^{-1} even when probed at early time. The exception is the 367.5 cm^{-1} band which is shown in Fig. 8 and clearly exhibits sharp structure at early and late time, indicating significantly slower IVR for this band. Thus we see again the mode specific redistribution rates.

The MATI spectrum of the 399 cm^{-1} band of the Ib isomer was also obtained at early and late time and is shown in Fig. 8. The early time spectrum shows sharp structure exactly where it is expected for the 399 cm^{-1} band of isomer Ib and the lack of intermolecular modes to the blue further confirms the Ib assignment. At late time, broader structure to the red appears as the sharp peak is diminished. Surprisingly the broad structure is not where it would be expected for the Ib isomer which would be at 29 525 cm^{-1} (indicated by an arrow in Fig. 8). Instead, it is consistent with the redistributed structure of isomer Ia (indicated by the dotted line in Fig. 8). This will be discussed further below.

3. 700 cm^{-1} region

In this region the vibrational energy is sufficient to dissociate one Ar from each complex as was shown above in

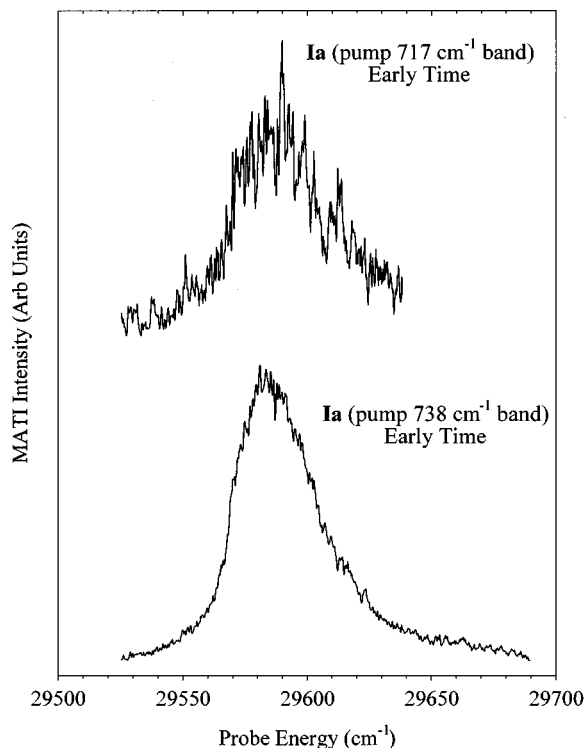


FIG. 9. Nanosecond MATI spectra obtained by pumping the Ia complex isomer 717 and 738 cm^{-1} bands. In this case the MATI signal is obtained by gating on the monomer mass which is the product of the dissociation. No reactants were observed, indicating rapid dissociation. The spectra width is due to rotational excitation in the monomer reaction product.

the mass resolved REMPI spectra. Here we focus on the dynamics of the dissociation in S_1 as measured by MATI spectroscopy. Measuring dissociation of the $n=1$ cluster is often more difficult than the $n=2$ cluster because the product of the dissociation is the monomer which is present in such abundance that background excitation can sometimes compete with the measured product. Also, when measuring the dissociation of the $n=2$ cluster to $n=1$ there is virtually no background due to the fact that the $n=1$ complex at the same energy also dissociates to the monomer.

Dissociation of the $n=1$ Ia complex was measured by nanosecond MATI probing at the 717 and 738 cm^{-1} bands. Figure 9 shows the MATI spectra of the monomer reaction products. No MATI [or multiphonon ionization (MPI)] signal assigned to the $n=1$ complex could be detected at the $n=1$ mass channel, even at early time. The lack of observation of MATI signal in the $n=1$ channel does not necessarily give information about the S_1 dynamics since dissociation may also take place in the ion (or more appropriately the ion core of the high n Rydbergs) during the MATI waiting period. However, the monomer MATI signal can give information about whether dissociation occurs in S_1 or the ion by analysis of the spectral signature. The spectra reveal no structure due to the $n=1$ complex confirming that dissociation occurred rapidly in S_1 . The product monomer MATI spectra are broad due to the rotational excitation from the reaction. These broad spectra are the signature of product monomers as opposed to background bands. Picosecond transients could not be obtained for these bands due to the

presence of a large monomer background signal which could not be effectively eliminated. Surprisingly the $n=2$ complex of the same bands could be measured with the picosecond system since any $n=1$ background was eliminated at the energy by dissociation to the monomer.

Dissociation of the $n=2$ species is more interesting due to the possibility of either of the two Ar atoms dissociating to a number of $n=1$ isomer products. The S_1 REMPI spectrum for the $n=2$ complex in this region can only be observed by monitoring the $n=1$ product mass channel. A total of five bands in this region have been further investigated with MATI spectroscopy. These include the IIa isomer bands at 668, 717, and 738 cm^{-1} and the IIb isomer 717 and 738 cm^{-1} bands. The MATI spectra obtained when pumping each of these bands (at early and late time) was identical and led to a broad peak in the $n=1$ mass channel centered at 29 550 cm^{-1} . The possible dissociation pathways are discussed below.

IV. DISCUSSION

A. Geometry of phenyl fluorene

The most important structural element for the purposes of this study is the torsional angle of the phenyl with respect to the fluorene plane. As mentioned, the *ab initio* calculations determined the phenyl group to be perpendicular to the fluorene plane resulting in C_s symmetry. This is critical in the structure of the Ar complexes because it determines how many distinct isomers can exist, particularly if we consider binding on the same side as the phenyl group. We cannot determine the structure experimentally with our data set but clues can be considered. For C_s geometry several of the low frequency vibrational modes involving phenyl motion are expected to be asymmetric and so may be absent in the spectrum. Two of the three lowest frequency modes calculated for the ground state are asymmetric, namely the phenyl wag along the long axis at 80 cm^{-1} , and the phenyl torsion at 98 cm^{-1} . The third symmetric mode is a phenyl out of plane wag, also at 98 cm^{-1} . Experimentally, one low frequency mode is observed at 47 cm^{-1} in S_1 and 42 cm^{-1} in the cation. However, since the mode cannot be unambiguously assigned, no inference on the molecular symmetry can be made. Measurement of the ground state frequency of this mode and comparison to the calculated values could help in the assignment. As mentioned above, the 209 cm^{-1} band in S_1 may correlate with the overtone of the phenyl torsion, which would support the C_s assignment, since the fundamental is missing from the spectrum.

C_s symmetry is consistent with the assignment of the Ar cluster structures. In particular there is only one $n=1$ structure which has an argon on the phenyl side. Atom-atom calculations with the phenyl twisted indicated two stable, but inequivalent, binding sites on the phenyl side of the fluorene.

B. Occurrence of multiple isomers

The observation of multiple isomers in PF-Ar $_n$, even for $n=1$, presents interesting opportunities for studying site specific properties of these types of clusters. Although there is a great amount of data now on vdW molecules, it is still

difficult to determine when, and under what conditions, multiple isomers may exist. The kinetics of the cooling process and the barrier heights to isomer conversion^{15,18} clearly play an important role which limits the applicability of thermodynamic arguments.

Presumably what is required for the observation of multiple isomers are relatively deep potential minima separated by significant potential barriers. In this study we have shown that one can “design” a system such as PF which offers multiple, asymmetric binding sites. Furthermore, once the individual isomers are identified the larger cluster structures can be “constructed” from the different isomers of the smaller species. Thus in this case the additivity rules work particularly well.

C. Isomer and band specific IVR

An important measurement in this work is the dramatically different rates for redistribution of the Ia and Ib isomers. For the 184 cm⁻¹ band, Ia exhibits redistribution with a rate of 1300 ps, while the Ib isomer shows no signs of redistribution at all. The difference between the two isomers continues for the 399 cm⁻¹ band where Ib does undergo redistribution but measurably slower than the Ia isomer (140 ps) for the same band.

One example of similar behavior has been reported in the literature which we are aware of. This is the perylene–Ar₂ system studied by Topp *et al.*,¹⁰ where they observed different degrees of spectral broadening for the 353 cm⁻¹ band for each of the two isomers assigned as (2|0) and (1|1). As perhaps one might expect the (2|0) isomer, with both argons on the same side, exhibited faster IVR dynamics probably due to the additional low frequency modes associated with the Ar–Ar interaction.

In the PF–Ar₁ case the different rates must be due to the different coupling of the vdW modes of the system to the chromophore vibrations rather than a density of states argument. For this particular system the two isomers differ in being on the same (Ia) or opposite (Ib) sides of the fluorene plane with respect to the phenyl group. As determined by the *ab initio* calculations, the three lowest frequency vibrations (in the ground state) are two phenyl wagging modes at 80 and 98 cm⁻¹ and the phenyl torsion at 98 cm⁻¹. These large amplitude motions undoubtedly couple more directly to the Ar motions (~20 cm⁻¹ bends, ~40 cm⁻¹ stretch) when the Ar is on the same side of the fluorene plane. The atom–atom calculations show that there is a large interaction between the Ar and the phenyl ring in the Ia isomer, whereas this interaction is almost zero in isomer Ib. This enhanced coupling is responsible for the accelerated redistribution of the Ia isomer. Conversely, this observation can be used to support the assigned structures of the isomers.

In addition to isomer specificity, the redistribution of the Ia isomer is shown to depend on the particular vibration excited in the chromophore and not just the total energy. This is evidenced by the closely spaced bands at 184, 205, and 215 cm⁻¹. Within this group the 184 cm⁻¹ band is observed to redistribute, but relatively slowly, with a time constant of 1300 ps. Nanosecond MATI spectra clearly show the 205 cm⁻¹ band redistributing more quickly but with discern-

able sharp structure still observed at early probe delay. The 215 cm⁻¹ band is completely redistributed, even at the earliest nanosecond probe delay. However, the band at 367.5 cm⁻¹ again shows slow redistribution. All other bands in the 400 cm⁻¹ region exhibit rapid redistribution. Mode specificity is well documented in other systems such as *p*-difluorobenzene–Ar³² and tetrazine–Ar,³³ and this is another clear example.

D. IVR and interconversion of isomers Ia and Ib

One of the interesting questions is at what excess energy, if any, do the isomer structures begin to interconvert? As shown above in the 200 cm⁻¹ region, the isomer Ia shows extensive redistribution but there is no evidence of MATI intensity which would be associated with population of the Ib structure, which would be expected to appear at ~29 525 cm⁻¹. The position of the expected Ib structure must be estimated since redistribution of Ib at the 200 cm⁻¹ level is not observed. Interconversion of the two isomers at the 200 cm⁻¹ level is not expected since it involves surface crossing, which for the related fluorene–Ar was calculated to require 260 cm⁻¹.

In the 400 cm⁻¹ region interconversion of Ia and Ib is expected to be energetically possible, particularly since this is close to the dissociation limit. The MATI spectra of the 367.5, 381, 388.5, and 399 cm⁻¹ bands of Ia all show redistribution with a pattern similar to that of the 200 cm⁻¹ Ia band but somewhat broader. The only feature in this region assigned to isomer Ib is shown in Fig. 8 at early and late time. Broad redistributed structure is clearly observed but the band shape and position are somewhat skewed by residual sharp structure. By carefully fitting this band the sharp structure was removed, leaving a clearer indication of the structure of only the redistributed product (the fitting results are not shown in Fig. 8). The resulting band is identical to the redistributed structure measured for the Ia isomer and shifted ~25 cm⁻¹ to the blue of where the redistributed structure of Ib would be expected. The conclusion here is that upon redistribution the Ib structure rapidly undergoes an Ar surface crossing to isomerize to the Ia structure. The dominance of the redistributed structure by the Ia isomer is then ascribed to the greater stability of this isomer and its significantly larger density of states compared to Ib. The added stability of the Ia is consistent with the fact that the Ia structure is more prominent in the S₁ excitation spectrum by a factor of 4.

E. Product channel identification in the *n*=2 dissociation

The dissociation of the *n*=2 complex, isomers IIa, IIb, and IIc, from bands in the 700 cm⁻¹ region raises some very interesting issues. First, each reactant may have two distinct Ar atoms providing two possible reaction channels. Second, the *n*=1 product has two isomeric forms which may be accessible from one or both of the reaction channels. In a recent publication¹⁵ we have demonstrated how fluorene–Ar₅ dissociated to two distinct *n*=4 isomer products. Unfortunately, only IIa and IIb had sufficient intensity to study at higher excess energy and these isomers have both been as-

signed as having two argons on one side (the side with the phenyl substituent). The binding sites on a single side are only separated by small barriers so, even upon modest excitation, the argons are expected to be labile. For excitation of all the bands in this region, for isomers IIa and IIb, dissociation was observed to occur rapidly and no MATI signal could be ascribed to the reactants even at early time. The product $n=1$ MATI spectra were observed, confirming rapid dissociation. All of the product spectra were identical, independent of the $n=2$ band excited, and the product is assigned as the Ia isomer with extensive redistribution. Given the excitation of $\sim 700\text{ cm}^{-1}$ and the S_1 binding energy of $\sim 500\text{ cm}^{-1}$, the products are expected to have $\sim 200\text{ cm}^{-1}$ excess energy. In fact, the product spectra are identical to the redistributed Ia at 200 cm^{-1} excess energy. No evidence is seen for production of isomer Ib. This is not surprising if the structural assignments are correct because Ib has an argon on the opposite side so it cannot be produced directly from dissociation of IIa or IIb, nor can it be produced in surface crossing from the product Ia since it has insufficient energy to overcome the barrier. The dissociation dynamics then further support the isomer structural assignments.

V. CONCLUSIONS

The monomer of PF has been characterized by *ab initio* calculations which establish the geometry of the plane of the phenyl group as being perpendicular to the fluorene plane giving an overall geometry of C_s .

An important result of this work is that different isomers of aromatic-Ar vdW molecules, and presumably other related systems, can easily be formed and remain stable in a supersonic expansion so long as the barriers for the interconversion are large enough to prevent cooling to the lowest isomer structure. Although these complexes have similar binding energies, it has been shown that the coupling between the chromophore and Ar intermolecular vibrations is dependent on the Ar binding site. This is manifest by different rates for vibrational redistribution in different isomers when excited to the same vibronic band in S_1 . Mode dependence of the redistribution is also demonstrated within a particular isomeric structure.

ACKNOWLEDGMENTS

We would like to thank Professor George Petersson and David Malick for providing the computational resources and expert advice for the *ab initio* calculations. We gratefully acknowledge the NSF for financial support of this project under Grant No. CHE-9523575.

¹K. R. Leopold, G. T. Fraser, S. E. Novick, and W. Klemperer, Chem. Rev. **94**, 1807 (1994); S. E. Novick, Bibliography of Rotational Spectra of Weakly Bound Complexes (1998). Electronic updates are available from the author upon request at snovick@wesleyan.edu and on the web at <http://www.wesleyan.edu/chem/bios/vdw.html>

- ²R. E. Miller and L. Pedersen, J. Chem. Phys. **108**, 436 (1998); D. T. Anderson, S. Davis, and D. J. Nesbitt, *ibid.* **107**, 1115 (1997).
- ³W. E. Sinclair and D. W. Pratt, J. Chem. Phys. **105**, 7942 (1996); B. B. Champagne, J. F. Pfanstiel, and D. W. Pratt, *ibid.* **102**, 6432 (1995); R. Sußmann and H. J. Neusser, Chem. Phys. Lett. **211**, 46 (1994); Th. Weber and H. J. Neusser, J. Chem. Phys. **94**, 7689 (1991); W. L. Meerts, W. A. Majewski, and W. M. van Herpen, Can. J. Phys. **62**, 1293 (1984).
- ⁴A. Heikal, L. Banares, D. H. Semmes, and A. H. Zewail, Chem. Phys. **157**, 231 (1991).
- ⁵M. C. R. Cockett, K. Okuyama, and K. Kimura, J. Chem. Phys. **97**, 4679 (1992).
- ⁶N. Ben-Horin, U. Even, J. Jortner, and S. Leutwyler, J. Chem. Phys. **97**, 5296 (1992).
- ⁷M. Mons, A. Courty, M. Schmidt, J. Le Calve, F. Piuze, and I. Dimicoli, J. Chem. Phys. **106**, 1676 (1997).
- ⁸P. Parneix, P. Brechignac, and F. G. Amar, J. Chem. Phys. **104**, 983 (1996).
- ⁹N. Ben-Horin, U. Even, and J. Jortner, J. Chem. Phys. **97**, 5988 (1992).
- ¹⁰M. M. Doxtader, I. M. Gulis, S. A. Swartz, and M. R. Topp, Chem. Phys. Lett. **112**, 483 (1984).
- ¹¹T. Troxler, R. Knochenmuss, and S. Leutwyler, Chem. Phys. Lett. **159**, 554 (1989).
- ¹²T. Troxler and S. Leutwyler, J. Chem. Phys. **95**, 4010 (1991); **99**, 4363 (1993).
- ¹³J. Bosiger, R. Bombach, and S. Leutwyler, J. Chem. Phys. **94**, 5098 (1991).
- ¹⁴X. Zhang, J. D. Pitts, R. Nadarajah, and J. L. Knee, J. Chem. Phys. **107**, 8239 (1997).
- ¹⁵J. Pitts and J. L. Knee, J. Chem. Phys. **108**, 9632 (1998).
- ¹⁶S. S. Ju, P. Y. Cheng, M. Y. Hahn, and H. L. Dai, J. Chem. Phys. **103**, 2850 (1995); L. Lapierre, D. Frye, and H. L. Dai, *ibid.* **96**, 2703 (1991).
- ¹⁷J. R. Johnson, K. D. Jordan, D. F. Plusquellic, and D. W. Pratt, J. Chem. Phys. **93**, 2258 (1990); C. Lakshminarayanan, J. M. Smith, and J. L. Knee, Chem. Phys. Lett. **182**, 656 (1991).
- ¹⁸A. R. Potts and T. Baer, J. Chem. Phys. **108**, 869 (1998).
- ¹⁹M. Mandziuk and Z. Bacic, J. Chem. Phys. **98**, 7165 (1993).
- ²⁰L. Zhu and P. M. Johnson, J. Chem. Phys. **94**, 5769 (1991).
- ²¹X. Zhang and J. L. Knee, Faraday Discuss. **97**, 299 (1994).
- ²²*Femtosecond Chemistry*, edited by Jörn Manz and Ludger Wöste (VCH, Weinheim, and VCH, New York, 1995), Chap. 4.
- ²³W. C. Wiley and I. H. McLaren, Rev. Sci. Instrum. **26**, 1150 (1955).
- ²⁴GAUSSIAN 94, Revision D.4, M. J. Frisch, G. W. Trucks, H. B. Schlegel, P. M. W. Gill, B. G. Johnson, M. A. Robb, J. R. Cheeseman, T. Keith, G. A. Petersson, J. A. Montgomery, K. Raghavachari, M. A. Al-Laham, V. G. Zakrzewski, J. V. Ortiz, J. B. Foresman, J. Cioslowski, B. B. Stefanov, A. Nanayakkara, M. Challacombe, C. Y. Peng, P. Y. Ayala, W. Chen, M. W. Wong, J. L. Andres, E. S. Replogle, R. Gomperts, R. L. Martin, D. J. Fox, J. S. Binkley, D. J. Defrees, J. Baker, J. P. Stewart, M. Head-Gordon, C. Gonzalez, and J. A. Pople, Gaussian, Inc., Pittsburgh, PA, 1995.
- ²⁵A. D. Becke, J. Chem. Phys. **98**, 5648 (1993).
- ²⁶M. Van Meerssche, G. Germain, J. Declercq, D. Lloyd, and D. J. Walton, Cryst. Struct. Commun. **8**, 635 (1979).
- ²⁷Hypercube, Waterloo, Ontario, Canada.
- ²⁸X. Zhang, J. M. Smith, and J. L. Knee, J. Chem. Phys. **97**, 2843 (1992).
- ²⁹D. F. Kelley and E. R. Bernstein, J. Phys. Chem. **90**, 5164 (1986).
- ³⁰T. Baer and W. L. Hase, *Unimolecular Reaction Dynamics: Theory and Experiment* (Oxford University Press, New York, 1996), p. 393.
- ³¹J. F. Kauffman, M. J. Cote, P. G. Smith, and J. D. McDonald, J. Chem. Phys. **90**, 2874 (1989).
- ³²K. W. Butz, D. L. Catlett, Jr., G. Ewing, D. Krajnovich, and C. S. Parmenter, J. Phys. Chem. **90**, 3533 (1986).
- ³³D. V. Brumbaugh, J. E. Kenny, and D. H. Levy, J. Chem. Phys. **78**, 3415 (1982); M. Heppener, A. G. M. Kunst, D. Bebelaar, and R. P. H. Rettschnick, *ibid.* **83**, 5341 (1985); P. Weber and S. A. Rice, *ibid.* **88**, 6120 (1989).